

## ABSTRACT

The Hubble Space Telescope (HST) is one of NASA's most productive astronomical observatories. Launched in 1990, the HST continues to gather scientific data to help scientists around the world discover amazing wonders of the universe. To maintain HST in the fore front of scientific discoveries, NASA has routinely conducted servicing missions to refurbish older equipment as well as to replace existing scientific instruments with better, more powerful instruments. In early 2002, NASA will conduct its fourth servicing mission to the HST. This servicing mission is named Servicing Mission 3B (SM3B). During SM3B, one of the major refurbishment efforts will be to install new rigid-panel solar arrays as a replacement for the existing flexible-foil solar arrays. This is necessary in order to increase electrical power availability for the new scientific instruments.

Prior to installing the new solar arrays on HST, the HST project must be certain that the new solar arrays will not cause any performance degradations to the observatory. One of the major concerns is any disturbance that can cause pointing Loss of Lock (LOL) for the telescope. While in orbit, the solar-array temperature transitions quickly from sun to shadow. The resulting thermal expansion and contraction can cause a "mechanical disturbance" which may result in LOL. To better characterize this behavior, a test was conducted at the European Space Research and Technology Centre (ESTEC) in the Large Space Simulator (LSS) thermal-vacuum chamber. In this test, the Sun simulator was used to simulate on-orbit effects on the solar arrays.

This paper summarizes the thermal performance of the Solar Array-3 (SA3) during the Disturbance Verification Test (DVT). The test was conducted between 26 October 2000 and 30 October 2000. Included in this paper are:

- A brief description of the SA3's components and its thermal design;
- A summary of the on-orbit temperature predictions;
- Pretest thermal preparations;

- A description of the chamber and thermal monitoring sensors;
- Presentation of test thermal data results versus flight predictions;

## 1. INTRODUCTION

The SA3 is scheduled for launch as part of the HST Servicing Mission 3B (SM3B) in November 2001. During SM3B, the SA3 will be changed out replacing the existing Solar Array-2 (SA2).

The primary objective in replacing the solar-array panels is to increase power capability that the solar arrays can provide to the Hubble Space Telescope. The SA2 currently on HST was constructed using silicon cells. Under this construction, the SA2 was capable of producing approximately 2500-Watt to be used by the HST. This power-producing capability of the SA2 has decreased over time due to environmental degradation and is no longer sufficient for HST.

The HST design power-usage guideline for the axial instruments was to have one axial instrument in operate mode consuming no more than 150-Watt, one radial instrument in operate mode consuming no more than 150-Watt and three other instruments in hold mode at no more than 58-Watt each. During Servicing Mission 2 (SM2), more advanced science instruments were installed onto HST. The more powerful instruments increased power requirement by 150-Watt. This trend of increasing power requirements will continue with the new instruments to be installed in SM3B in 2002 and Servicing Mission 4 (SM4) in 2004. With the final complement of scientific instruments and housekeeping electronics, the value of energy demand by HST will be as much as 2650-Watt. The new rigid-panel solar arrays with more efficient solar cells will be able to produce a minimum of 2800-Watt.

As with any newly designed hardware to be installed onto the HST, the engineering team must ensure that the solar arrays will not cause any degradation in HST observatory performance. One of the major engineering issues that the HST solar-array team must

address is the disturbance issue. Large disturbances can cause the observatory to lose its pointing lock on the targeted star, interrupting science acquisitions. For the solar arrays on HST, disturbances are primarily caused by rapid change in temperature while the observatory is moving from the sunlit portion of its orbit around the earth into eclipse or vice versa. Within a matter of a few minutes, the average temperature on the solar-array panels can change as much as 160 degrees Celsius. This temperature change will cause various rates of thermal expansions and contractions on different parts of the solar arrays. The resulting thermal expansion and contraction can cause a "snap" on the arrays that may cause a Loss of Lock (LOL) in the observatory.

## 2. TEST SET-UP

The SA3 thermal test configuration is shown in Figure 1, comprising of both flight hardware and ground support equipment (GSE) components.

### 2.1 SA3 Flight Hardware

The **Solar Array Drive Adapter (SADA)**, developed by ESA, is the section of the assembly that connects the SA3 mast assembly to the Hubble Space Telescope. The male end of the SADA is connected to the mast; the female end is attached to HST.

The **Solar Array Drive Mechanism (SADM)**, also developed by ESA, is a cylindrical device that contains a motor, enabling the solar-array mast to rotate. The SADM is covered by a metal shield and a MLI blanket. Thermostatically-controlled redundant survival heaters are located within the SADM for temperature control. The thermostat for the primary 10-Watt heater closes at  $-27^{\circ}\text{C}$  and opens at  $-13^{\circ}\text{C}$ . The secondary 10-Watt heater's on and off set points are  $-33^{\circ}\text{C}$  and  $-18^{\circ}\text{C}$ , respectively. Two sets of SADM cables and connectors carry power from the solar arrays to the telescope.

The **Coupler** is a titanium spool to which electrical connectors from the solar arrays are attached. Two gold-anodized handles and the electrical connectors protrude through the blanket that covers the coupler.

The **Damper** is a titanium spool with visio-elastic material (VEM) sandwiched between titanium shear laps. This device increases the damping of the solar arrays, providing pointing stability margin. Thermostatically-controlled heaters are located within the damper for temperature control. The thermostat for the primary 25-Watt heater closes at  $+10^{\circ}\text{C}$  and opens at  $+15^{\circ}\text{C}$ . The secondary 10-Watt heater's on and off set points are  $+4^{\circ}\text{C}$  and  $+10^{\circ}\text{C}$ , respectively. A MLI blanket completely surrounds the damper to reduce heater duty cycles during on-orbit operation.

The **Mast** is a M55J graphite-composite cylinder with two gold-anodized handles protruding through a MLI blanket.

The **Panel Support Structure (PSS)** is the mounting frame for the solar panels. The major elements are fabricated of Aluminum-Lithium Alloy X2096. Flexures are located at twelve locations (3 per panel) to displace thermal distortion. The PSS is covered with MLI, except the hinges which are covered with silver-Teflon tape.

Four **Solar-Array Panels** are used in the SA3 assembly. These panels incorporate the Iridium<sup>®</sup> design with 1000 Gallium Arsenide on Germanium solar cells per panel. The cells are attached to a Kapton face sheet of an aluminum honeycomb core. The anti-sun sides of the panels are white Tedlar to serve as radiators to space.

### 2.2 Ground Support Equipment (GSE)

The **Pedestal** is used to elevate and support the SA3 mast and panel assembly into the Sun simulator beam. Seven heater circuits on the pedestal and a MLI cover are used to maintain a steady temperature.

The **SADM Heater Plate** is used to simulate the warm HST body and to maintain realistic SADM and Damper flight-heater duty cycles during the test

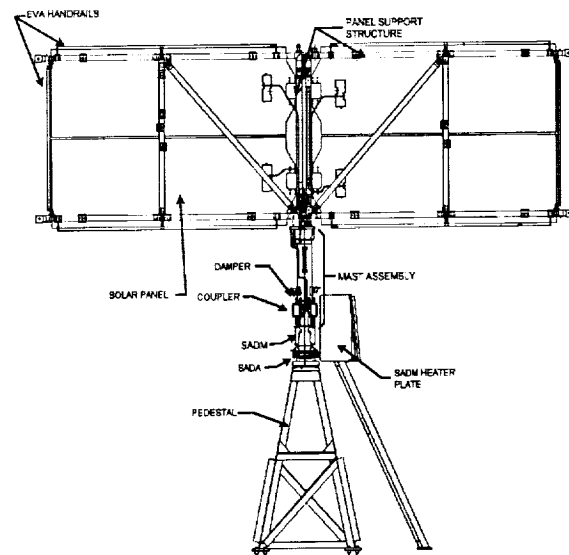


Fig. 1. Test Setup

## 3. ON-ORBIT TEMPERATURE PREDICTIONS

The orbital attitude and environment, material properties, internal power dissipation and heater performance influence the temperature variations of the SA3 panel, PSS and mast assemblies. Orbital attitude includes sun-orbit or beta angle that varies  $\pm 52.2^{\circ}$  for

HST and sun angle, which is allowed to roll  $\pm 30^\circ$  about a vector perpendicular to the mast and parallel to the solar panels during nominal operations. The orbital environment including solar flux, albedo and Earth-infrared flux are summarized in Table 1.

Table 1: Environmental Flux

Unit:	Solar Flux		Earth Flux	
	W/m <sup>2</sup>	Btu/hr-ft <sup>2</sup>	W/m <sup>2</sup>	Btu/hr-ft <sup>2</sup>
Hot case	1440	457	272	86.5
Cold case	1264	401	197	62.5

Albedo Flux is 35% of Solar Flux in Hot Case  
And 25% of Solar Flux in Cold Case

Material finishes of the various SA3 components are assigned the values of absorptivity ( $\alpha$ ) and emissivity ( $\epsilon$ ) shown in the Table 2. The majority of the components are covered in MLI. The beginning-of-life (BOL) numbers are based on actual measurements and the end-of-life (EOL) properties are based on empirical projections or measurements made on samples retrieved from the observatory after nearly 10 years of service.

Table 2: Surface Properties

	BOL (Cold)		EOL (Hot)	
	$\alpha$	$\epsilon$	$\alpha$	$\epsilon$
S/A Back	.47	.85	.47	.85
Solar Cells	.87	.85	.87	.85
Handrails	.47	.87	.47	.87
Al/Tef Tape	.12	.05	.14	.03
Al/Tef MLI	.12	.78	.25	.78
Ag/Tef Tape	.08	.78	.18	.75

Internal power dissipations were measured during electrical tests of the SA3. The major power dissipater is the SADM that dissipates 2-Watt worst case (hot). For cold-case computations no power dissipation was assumed.

And finally, the heater design such as set point selection, primary and secondary-circuit parameters (which were mentioned in the Test Setup Section 2) determine the amount of heat introduced by the heaters. The predicted duty cycles of the primary heaters are of particular interest, as they are required to remain below 70%. Secondary-heater circuits should not be activated even in the cold case.

The resulting temperatures are shown in the following two charts. Figure 2 shows a hot-case prediction of solar-panel and PSS temperatures. The first of the four lines represent the most extreme temperatures of the SA3, front-panel temperatures. The solar cells are placed on a thin Kapton face sheet attached to a low-density aluminum-honeycomb core. The back of the

panel responds slower to the heat flux soaking from the front. In addition, the white Tedlar surface on the back has a strong coupling to space and cools the solar panel throughout the illuminated portion of the orbit.

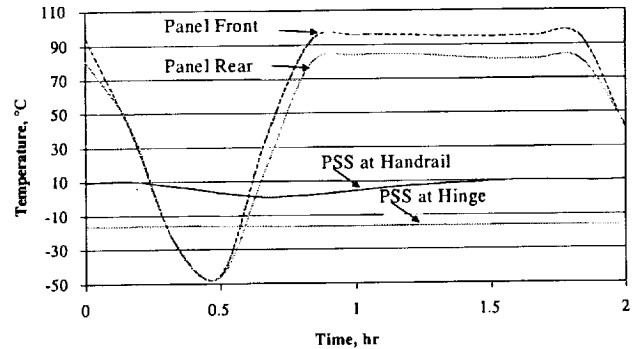


Fig. 2. Panel & PSS Flight Temperatures

The other two temperature profiles in Figure 2 illustrate two very different responses of the PSS to its environment. These profiles are significant in as much as they introduce the majority of the thermally induced noise into the SA3 system. Notice that the area of the PSS closer to the handrails will experience a more extreme temperature swing than the area near the hinges. The PSS thermal-design strategy is to minimize temperature swing near the root (hinge), diagonal and center areas to reduce PSS contribution to overall SA3 noise.

The Mast, Damper, Coupler and SADM temperatures are shown in Figure 3. The Damper temperature profile shows heater operation (primary only) that may affect the low frequency movements of the SA3.

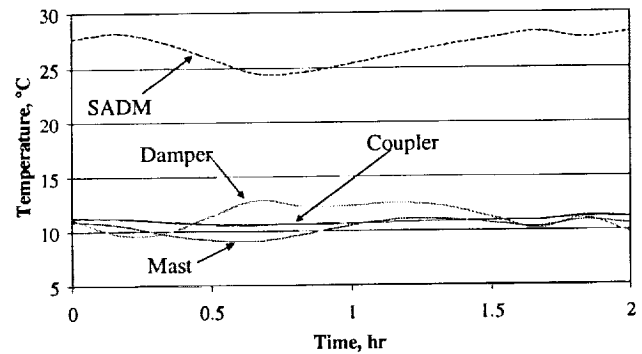


Fig. 3 Mast-Assembly Flight Temperatures

The Mast, Coupler and SADM show only flux-induced orbital temperature variations since heaters are not in operation. It should be noted that the SADM heaters have a  $-27^\circ\text{C}$  set point and are therefore used only as survival heaters.

Table 3 summarizes predicted SA3 orbital temperatures. The variation of these temperatures during an orbit is of particular interest for the DVT since relative

thermal expansion or contraction of major structural elements, such as the PSS, can produce LOL.

Table 3: Predicted Test and On-Orbit Temperatures

TC No.	Location	Operate Limits (°C)	Nominal Orbit		During the DVT	
			Min (°C)	Max (°C)	Min (°C)	Max (°C)
102	Panel 2 face	-85, 105	-64	81	-75	72
103		"	-52	98	-72	91
105		"	-5	84	-18	80
107	Panel 1 face	"	-55	90	-72	81
110		"	-5	84	-18	80
111		"	-66	81	-78	74
126	Panel 2 back	"	-66	56	-75	44
127		"	-52	84	-71	75
129		"	2	65	-11	63
131	Panel 1 back	"	-56	73	-74	38
132		"	-65	57	-73	46
134		"	2	66	-10	64
149	SADA cone	-55,+80	24	36	12	19
150	SADM T1	-55,+80	27	28	11	14
152	SADM T2	-55,+80	28	35	13	18
153	SADM shield	-55,+80	27	38	12	18
157	Mast Coupler	None	10	23	7	17
161	Damper	-70,+50	10	14	10	12
165	Mast tube	None	-4	1	-13	-5
173	Mast hinge	None	3	7	-16	-13
175	PSS, fixed	None	-18	-17	-19	-17
181			3	13	-20	-13
183	PSS, hinged	None	0	7	-16	-12
189			4	10	-25	-23

#### 4. DESCRIPTION OF THERMAL CHAMBER AND THERMAL MONITORING SENSORS

The LSS chamber at ESTEC has a usable volume of 9.5 meters in diameter and 10 meters in height. The chamber includes a Sun simulator (SUSI) with a 6-meter diameter beam capable of producing 2000 W/m<sup>2</sup> of illuminated energy at 5 meters from the source. Since the deployed solar arrays are wider than the SUSI beam it was necessary to mount the solar arrays at a 49° angle of incidence. This allowed all solar arrays to be illuminated by the SUSI. To prevent the solar arrays from exceeding their cold operating limit of -85°C, the shroud was held at -80°C. Using the afore mentioned conditions, the maximum SUSI intensity that would produce thermal and mechanical responses close to on-orbit predictions was calculated to be 1600 W/m<sup>2</sup>.

To adequately monitor the test configuration temperatures while minimizing the induced stresses caused by the weight of the thermal harness, the number of thermocouples was limited to 132. Two types of Copper-Constantan type-T thermocouples were used: fast and standard response. Twelve fast-response thermocouples, with .002" diameter wire, permit a resolution of one sample per second while the 120 standard-response thermocouples were used to recover data at one sample every two minutes. Figure

4 shows the location of the twelve fast-response thermocouples on the sun-facing and anti-sun-facing surfaces on Panel 2. Figures 4, 5, and 6 show typical locations of the standard-response thermocouples.

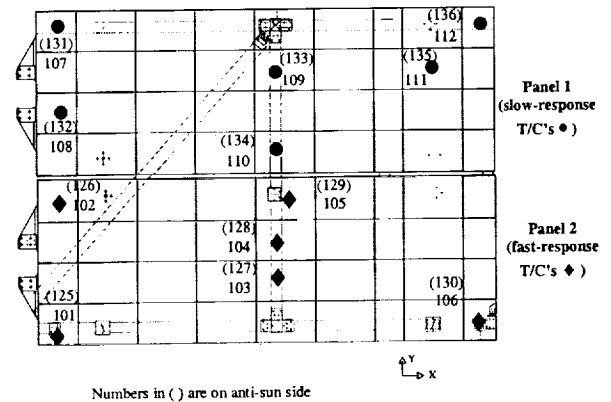


Fig. 4. Typical Solar-Panel Thermocouples

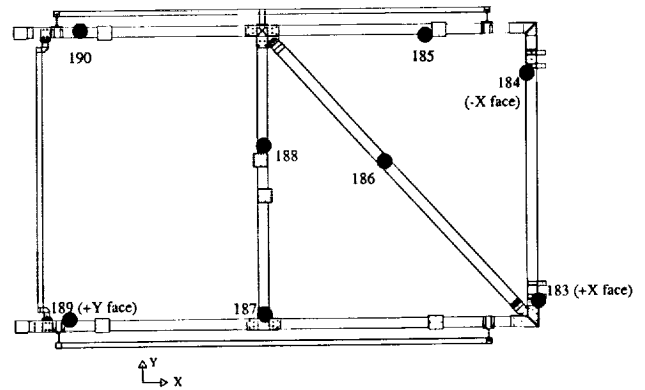


Fig. 5. Typical Panel Support Structure (PSS) Thermocouples

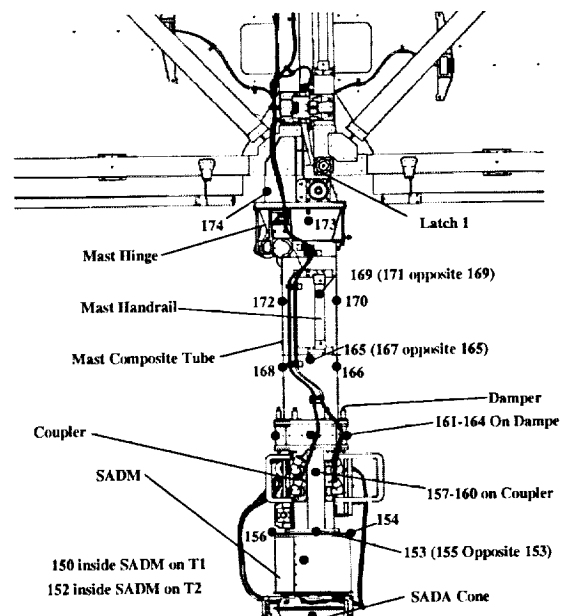


Fig. 6. Mast Assembly Thermocouples

A mathematical thermal model of the test set-up, including the solar arrays and the LSS, was constructed in Thermal Systems Synthesizer (TSS) and System Improved Numerical Differencing Analyzer (SINDA). Thermal predictions were generated for the different phases of the test and compared to the flight thermal-model predictions and are listed in Table 3. Prior to the orbit-transition phase of the DVT, a semi-thermal balance test was conducted to verify that the solar arrays would not exceed their temperature limits when the 1600 W/m<sup>2</sup> of simulated Sun illumination was applied. Since this was a semi-thermal balance and not the orbit-transition phase, 1200 W/m<sup>2</sup> of simulated Sun illumination was used.

## 5. THERMAL TEST DATA

The DVT was conducted over a period of 89 hours in the LSS chamber. While under vacuum, the SA3 wing was subjected to a contamination bake out, two thermal-balance points, and eighteen orbital cycles. The following are notable events during the test.

### 5.1 Thermal-Balance Test

The primary objective of the thermal-balance test was to make sure that the selected solar-intensity level to be used during the orbital-cycling portion of the test would not cause any component of the SA3 wing temperature to exceed their operational limits. A secondary objective was to fine-tune selected test parameters.

The first thermal-balance point was selected with the chamber shroud temperature at -80°C, the solar intensity at 1200 W/m<sup>2</sup> and the SADM heater-plate temperature at 60°C. With the allocated time of 4 days to complete the DVT, it became apparent that there was not enough time for all components to reach their thermal-balance temperatures. Because of this, a decision was made to limit the thermal-balance test to just the solar panels. The analyses predicted that the temperature on the panels were close to their upper limit of +105°C. It was also discovered in this test that the chamber shroud temperatures were not uniform. The distribution of the shroud temperatures varied from -80°C to -45°C. At the balance point, the temperatures of the sun sides of the solar panels ranged from +65°C to +80°C, approximately 25°C above predicted.

A second thermal-balance point was conducted to help determine the solar-panel temperature sensitivity with increasing solar intensity. To accomplish this objective, all environmental conditions were left the same except the solar intensity, which was increased to 1400 W/m<sup>2</sup>. At stability, the temperatures on the solar-panels increased by approximately 12°C.

At the end of the thermal balance test, it was concluded that the solar-panel temperatures were 25°C higher than predicted. This was believed to be caused by the warmer average shroud temperature. The PSS, SADM, Mast and Damper did not reach their balance temperatures. As a result, the calculated solar intensity for the orbital thermal-cycling portion of the test was reduced from 1600 W/m<sup>2</sup> to 1300 W/m<sup>2</sup> to compensate for the warmer chamber environment.

### 5.2 Orbital Thermal-Cycling Test

The remainder of the testing time was dedicated to the orbital thermal-cycling phase. Mechanical disturbance measurements caused by temperature changes of the SA3 in simulated flight conditions would be recorded for as many cycles as time permitted. The initial plan was to power on the SUSI, which provided simulated Sun flux at 1300 W/m<sup>2</sup> for a period of 60 minutes and power off for 30 minutes. The duration of the SUSI on/off cycle was compatible to HST's on-orbit experience. The chamber shroud temperature set point remained at -80°C. The on-orbit temperature prediction as discussed in Section 3 showed that the temperatures of the solar panels would vary from -70°C to +94°C over the course of an orbit. The PSS and the Mast were predicted to vary less than 5°C and 10°C, respectively.

It was anticipated that it would take as many as 10 cycles for components to settle into their on-orbit quasi-steady temperatures. The solar panels quickly achieved their repeatable temperatures due to their light mass and large exposed surface area. The resulting temperatures on the solar panels were -60°C to +83°C; less than the on-orbit predictions. In order to expand the range of temperature swing; on the hot side the solar intensity was increased to 1400 W/m<sup>2</sup>, and on the cold side the SUSI power off time was increased to 60 minutes. These changes were incorporated on cycle 6 of 18. This approach produced solar-panel temperatures of -70°C to +92°C, which matched well with the predictions.

The PSS, mostly covered with MLI, reached the on-orbit repeatable temperatures late in this phase around cycle 14. The majority of the PSS orbital temperature oscillations were as expected within ±5°C. However, there were exceptions. Sections of the PSS with mechanical connections to the solar panels tended to exhibit orbital-temperature swings larger than predicted. The most extreme swing recorded was 18°C. A sample of test data is shown in Figure 7.

The Mast test temperatures were well within the on-orbit predictions of 10°C day/night swing. Similar to the PSS, one section on the mast that had exposure to the environment showed a temperature oscillation of 20°C.

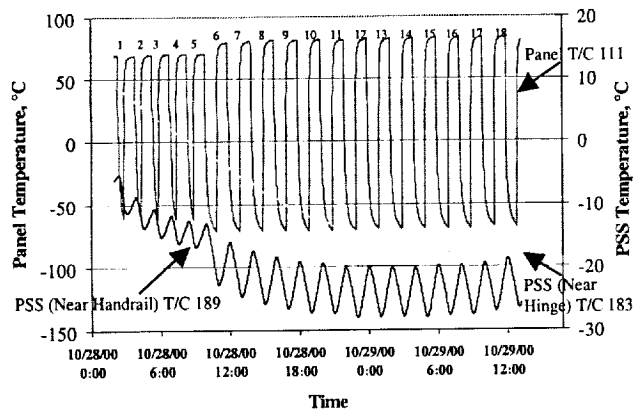


Fig. 7. Orbital Thermal Cycling

Throughout the orbital-cycling test, mechanical measurements were conducted to detect any disturbance from the solar arrays. Most of the data recorded indicated that the levels of disturbance were within the specifications for HST, however, on cycle 10, a high level of disturbance was measured. This data was referred to as a major event since it could cause LOL to HST. After reviewing the data of the event, it was believed that the disturbance was caused by the heater control of the pedestal. Up to this point, the pedestal still was cooling down from the contamination bake-out phase. Once the pedestal temperature cooled to within the thermal-control range, the heater circuit became active and the major disturbance event was recorded.

To confirm the theory that the pedestal heaters were the cause of the mechanical disturbance, the pedestal heaters were disabled during cycles 11 and 12 and no major events were recorded. Prior to the conclusion of the test, the pedestal heaters were once again enabled in an effort to duplicate the disturbance. Several events were recorded but none reached the same magnitude as the previous anomaly.

## 6. SUMMARY

To verify that the new rigid-panel solar arrays would not cause LOL to HST due to orbital-temperature variations, one wing of the SA3 was tested in the LSS chamber in the ESTEC facility. Over the four days of testing, the SA3 was subjected to a contamination bake-out, shortened thermal-balance tests, and 18 thermal-vacuum temperature cycles.

Analytical SINDA and TSS simulations were performed before the test to ensure that test goals were successfully met. These analyses included on-orbit predictions to set temperature targets to be achieved during the test.

During the thermal-balance test, it was discovered that the thermal chamber was not able to provide a uniform shroud temperature at  $-80^{\circ}\text{C}$ . This was believed to cause the SA3 temperatures to be generally higher than predicted, particularly the solar panels. It was also determined that with the limited test time, there was not sufficient time to conduct a full thermal-balance test. A shortened version of the thermal-balance test was conducted which mainly focused on the solar panels. From the results of the thermal-balance test, the calculated solar intensity to be used in the thermal-cycling test was lowered to compensate for the higher than expected average shroud temperature.

Eighteen on-orbit simulation temperature cycle tests were conducted. Some minor adjustments to the solar-intensity levels and the solar-off duration periods were made to achieve a better match of the test data with the on-orbit predictions. The test provided highly valuable data to both the thermal design and mechanical-disturbance investigation. A few sections of the PSS and the Mast that were exposed to the environment experienced larger than expected temperature swings from orbit night to orbit day. One major mechanical-disturbance event was recorded during the test that could potentially cause LOL to HST. This incident was believed to be caused by the heater control system on the pedestal. The data collected during the test will be used to ensure that the chance of LOL on HST caused by the SA3 orbital-temperature variations will be minimized or eliminated.

## 7. CONCLUSION

Detailed thermal simulations were key to the success of the DVT test. The simulations:

- Guided design of test and test hardware
- Ensured safety and integrity of flight hardware
- Allowed real-time updates of test parameters
- Are now test-correlated, proven to provide confidence of on-orbit SA3 performance.

## 8. REFERENCES

1. Test Plan for the Disturbance Verification Test of Solar Array 3, GSFC P-442-2536, September 2000.
2. Poinas P. and Gomez-Hernandez C., ESARAD Geometrical Mathematical Models of the Large Space Simulation Chamber, *Proceedings of the Third International Symposium on Environmental Testing for Space Programmes*, June 1997.
3. Solar Array 3 Critical Design Review Package, LMMS/P471291, March 1998.